

COMPARING THE PERFORMANCE OF HELICAL ANCHORS AND DIRECT-EMBEDDED PLATE ANCHORS IN COHESIONLESS SOIL FOR TOP-DOWN RETAINING WALLS STABILIZATION: AN EXPERIMENTAL STUDY

Mohammad-Emad Mahmoudi-Mehrizi¹ and Matin Jalali-Moghadam^{2*}

ABSTRACT

Mechanical reinforcements such as helical anchors, plate anchors, and direct-embedded plate anchors are implemented to stabilize different permanent and temporary retaining walls such as excavations and reinforced earth walls without grouting. Today, these anchors are widely used because of their high operation speed and the possibility of post-tension immediately after installation. In the present study, the performance of two common types of mechanical anchors, namely the helical anchor and direct-embedded plate anchors, is analyzed in the stabilization of retaining walls using physical modeling. In addition, the parameters including the number of the helices, shape and dimensions of anchor plates, and installation configuration of reinforcement are evaluated. The horizontal wall displacement was recorded by dial gauges installed in front of the facing and the critical slip surfaces of the mechanically stabilized earth walls or failure wedge were identified using Particle Image Velocimetry (PIV). Increasing the number of the screws in helical anchors from 1 to 2 and changing the circular and square plates from small to medium size led to a 60% increase in bearing stress of the strip footing. In comparison, increasing the number of screws from 2 to 3 and changing the circular and square plate anchors from medium to big size resulted in only 29% increase in the bearing stress. Although the number of reinforcements is equal in both diamond and square configurations, the diamond configuration showed considerably higher performance in controlling the displacement of wall crest than the square configuration.

Key words: Helical anchor, plate anchor, direct-embedded plate anchor, retaining wall, particle image velocimetry.

1. INTRODUCTION

An earth anchor is a device designed to support structures, most commonly used in geotechnical and construction applications. These anchors are divided into two main groups of grouted and mechanical anchors. The grouted anchors include bar or strand, which are mainly tensioned after grout injection. The mechanical anchors include helical anchors, plate anchors, and direct-embedded plate anchors. These two groups have their own advantages and disadvantages depending on their operational method and structural properties. The most important weaknesses of grouted anchors are:

- The lengthy time needed for grout settling and delay in post-tensioning operations
- The low speed of drilling in collapsible soils and the necessity of casing during the reinforcement installation
- Their longer effective length compared to mechanical anchors
- The complexity and big size of their installation equipment and machinery compared to mechanical anchors

- The difficulty of their installation in areas with limited access
- The possibility of their injection in marine and underwater projects

Helical anchors consist of a steel shaft with one or more helices (screws) welded to it (Fig. 1(a)). They are screwed into the ground using the hydraulic torque motors. The helical anchors and the direct-embedded plate anchors are installed in top-down order.

The direct-embedded plate anchors are threaded into the ground using a shaft. Then, after reaching the desired depth, the shaft is pulled out and the strand is tensioned to rotate the anchor plate to the final position under 90° angle (Fig. 1(b)). Duckbill, Manta ray, Stingray, and Driven Tipping Plate Earth anchors are the commercial names of some anchors that are used as the direct-embedded plate anchors.

To the best of our knowledge, a limited number of studies have been performed to stabilize retaining walls using helical anchors and plate anchors. Perko (1999) summarized applications of helical anchors used in retaining wall systems, which included the analysis of helical anchor bearing capacity and an example of designing the retaining wall. Deardorff *et al.* (2010) described the results of the preparation of instrumented helical soil nail wall. They also evaluated the designing and installation methods of the wall together with the initial results obtaining from instrumentation. Lutenneger (2011) studied the behavior of multi-helix anchors with the square shaft in sands using uplift tests on the real scale. Besides, in this study, the results were compared with those of commercially available three-helix anchors, in which the

Manuscript received March 18, 2019; revised August 7, 2019; accepted September 3, 2019.

¹ Ph.D. candidate, Geotechnical Engineering, Department of Civil Engineering, Campus International of Kharazmi University, Tehran, Iran.

^{2*} Master of Science (corresponding author), Geotechnical Engineering, Azad University, Central Tehran Branch, Tehran, Iran (e-mail: matin.jalali.m@gmail.com).

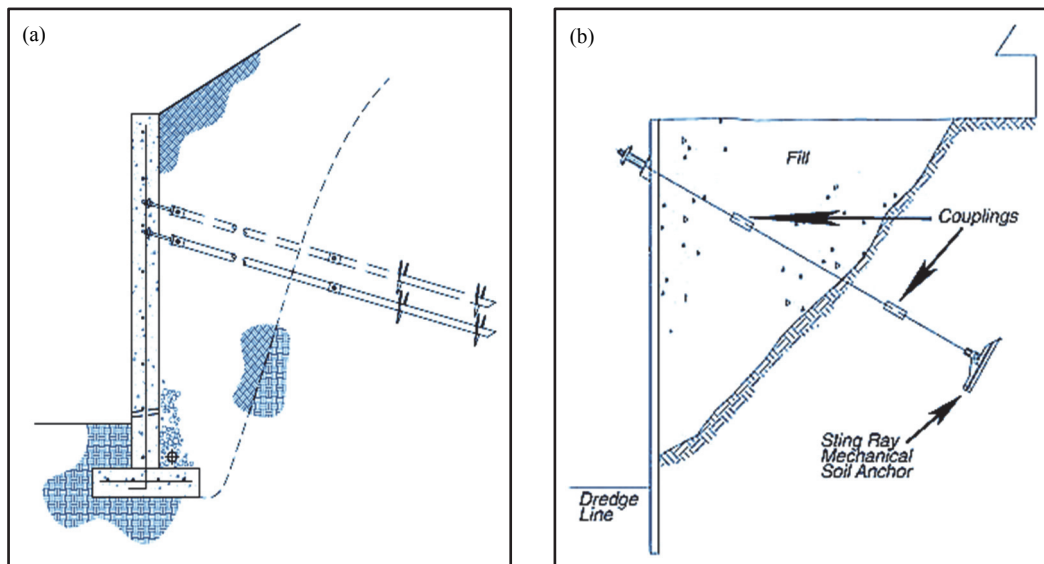


Fig. 1 The use of mechanical anchors in top-down retaining wall construction: (a) helical anchor (Perko 2009); (b) directly embedded plate anchor

diameter of the helix is increased in the shaft. Sharma *et al.* (2017) and Tokhi *et al.* (2016, 2017) performed comprehensive pullout tests on embedded helical soil nails in sandy soil. The results showed that the sliding mechanism is different from that of conventional soil nails and the pullout resistance is higher than conventional soil nailing. Also, in contrast with conventional soil nail, the tension bearing capacity of helical soil nail depends on surcharge pressure and failure planes are expanded in a certain radius from soil-nail interference (Tokhi *et al.* 2016, 2017). Sharma *et al.* (2017) used the number and diameter of helices, the pitch of the helix, and surface roughness of the nail shaft as variable parameters. The study indicated the significant effect of surface roughness of the shaft on the maximum pullout resistance of helical soil nail and the existence. Moreover, they reported a linear relationship between the maximum pullout force and surcharge pressure for all kinds of screw soil nail, which gives satisfying results in the Mohr-Coulomb failure criterion.

For the first time, Geddes and Murray (1996) evaluated the pullout behavior of plate anchor group in sandy soil. They showed that the bearing capacity of the plate anchor group is increased by increasing the distance of each plate. Sawwaf and Nazir (2006) investigated the behavior of vertical plate anchors buried in reinforced and unreinforced granular soils using the small-scale model tests. The results revealed that reinforcement significantly increases the stiffness of soil and pullout resistance of shallow anchor plates. Hanna *et al.* (2015) performed a comprehensive analytical and laboratory-based research to evaluate the pullout capacity of the inclined shallow single plate anchor in sand. After validating the developed theory with the experimental results and data obtained from the literature review, they developed the analytical model to provide information for a wide range of inclined anchors, soils, and geometries. To the best of our knowledge, only Moga-hadam *et al.* (2018a, 2018b) investigated the performance of mechanically stabilized earth walls using plate anchor reinforcements. They evaluated the effect of adding recycled crumb rubbers in backfill and the effect of changing the properties of plate anchor reinforcements on the whole stability of the retaining wall and the formation mechanism of failure wedge.

In several studies, only the number of screws and deformation of plate anchors on the bearing capacity have been evaluated and no study has investigated the effect of helical anchor group and direct-embedded plate anchors on the entire stability of retaining wall. Considering the studies of Clemence and Lutenegeger (2015) on subjects that should be studied in details, determining the behavior of helical anchor group and evaluating the behavior of these members on stabilization of retaining walls is one of the important issues that no certain ideas have been presented so far and should be investigated. Hence, in the present study, the behavior of two types of mechanical anchors is evaluated and compared. Next, the effects of the number of screws, changing the dimensions and shape of anchor plates, and their configuration on the retaining wall deformation and bearing stress of footing are studied. The results are presented with respect to horizontal displacement of wall crest, bearing stress of footing, and critical slip surface formation in the backfill.

2. THEORETICAL ASSESSMENT

The most typical methods to predict the pullout capacity of helical anchors are cylinder shear, individual bearing, and installation torque (experimental method). It was approved the higher compatibility of the experimental method compared to other methods. Nevertheless, it is suggested using cylinder shear and individual bearing methods to determine the minimum allowable area of screw and installation torque method to confirm the accuracy of bearing capacity (Hoyt 1989; Perko 1999). Boussinesq (1885)'s equation described the stress distribution in soil induced by applying load through a plate or buried footing. It is of note that in a multi-screw anchor installed in a homogenous soil with helices close together, the overlapping of plates can result in stress distribution and possible interference, thereby leading unpredicted failure. Therefore, the distance between helices should be observed. The large distance between the screws prevents the overlapping of the stress in the soil but leads to observing a very long helical anchor which is not economical. According to Boussinesq's theory, the stress value at a distance equivalent to screw diameter from the buried plates is 28% of the stress

on the plate surface. It should be noted that the stress value at distance equivalent to three times of screw diameter from buried plates is only 4% of the stress on the plate. The more distance from plate leads to an insignificant reduction in the stress value. Boussinesq's equation showed that the distance equivalent to three-time of screw diameter is a stress distribution-based solution (Fig. 2). Both cylinder shear and individual bearing methods present allowed failure mechanism for the distance equivalent to three-time of screw diameter. At distance lower than three-time of screw diameter, the cylinder shear controls the bearing capacity, while at higher distance individual bearing controls it.

The individual bearing method is based on an assumption that each helical plates are independent in soil (Fig. 3); therefore, their ultimate capacity of the anchor is the sum of the capacity of all individual helices (Stephenson 2003). This method is in agreement with the common bearing capacity theory developed by Terzaghi, Meyerhof, Hansen, and Vesic. Equations. (1) and (2) show the general form of this method, which is used for helical anchors.

$$Q_u = \sum_{i=1}^N Q_{hi} \quad (1)$$

$$Q_{hi} = q_{hi} \cdot A_{hi} \quad (2)$$

where Q_u is the ultimate capacity of the anchor, Q_{hi} is individual helix capacity, and q_{hi} is bearing capacity of soil that can be calculated by Eq. 3 (Perko 1999; Stephenson 2003):

$$q_{hi} = c_i N_c + \frac{1}{2} d_{hi} \gamma_i N_\gamma + \gamma_i H_i N_q \quad (3)$$

where three terms respectively are cohesion, friction angle, and surcharge to determine bearing capacity; c_i is soil cohesion; d_{hi} is helix diameter; γ_i soil unit weight; H_i the embedded depth of helix. Also, N_c , N_γ , and N_q are coefficients of bearing capacity for, cohesion, friction angle, and surcharge, *i.e.*, typically they are the reduced

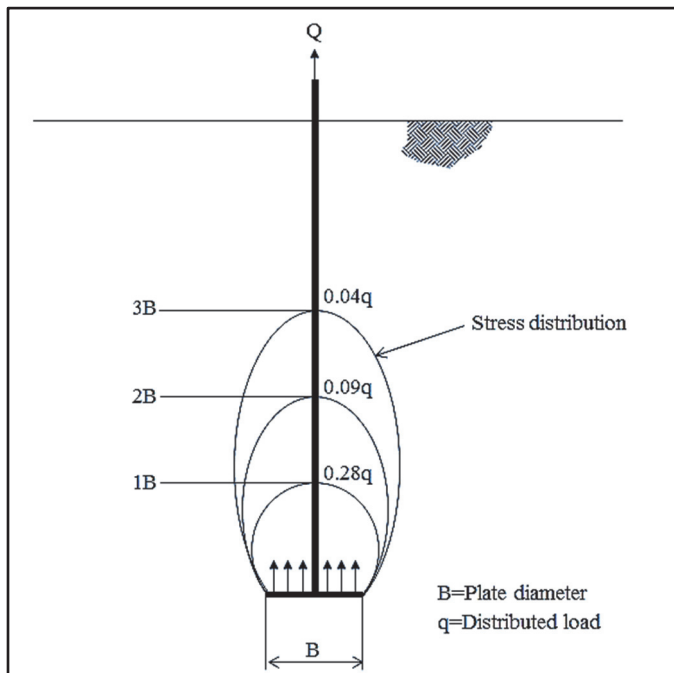


Fig. 2 The stress distribution above the deeply buried circular plate

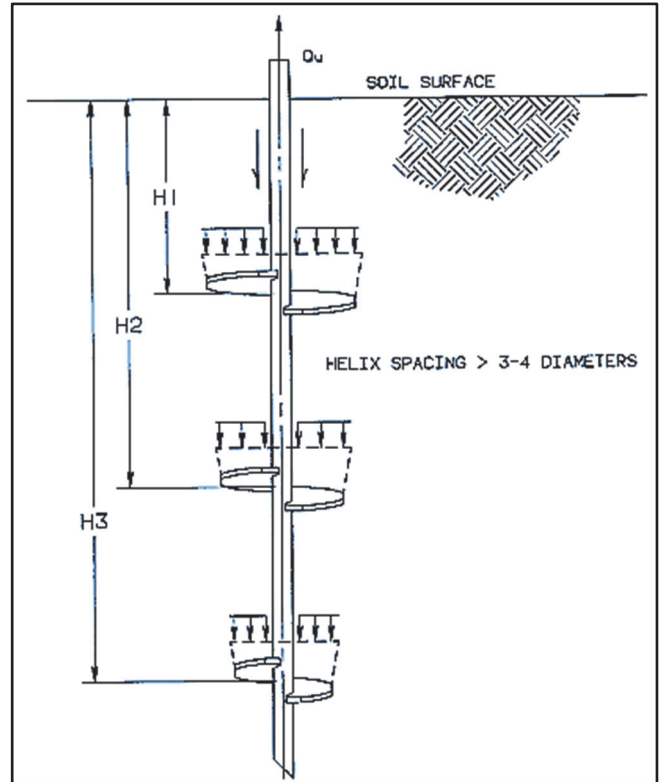


Fig. 3 The individual plate bearing capacity theory (Hoyt 1989)

coefficient of Meyerhof bearing capacity. When the helix diameter is small, N_γ plays a little role in bearing capacity. Since the diameter of the helix varies between 8 to 14 inches, ignoring N_γ seems logical (Stephenson 2003). Considering Eq. (3), the capacity of each anchor can be calculated by Eq. (4) (Perko 1999):

$$Q_u = \sum_1^N A_n (cN_c + \gamma_i H_i N_q) \quad (4)$$

For granular soils ($c = 0$), Eq. (4) is written as follows:

$$Q_u = \sum_1^N A_n (\gamma_i H_i N_q) \quad (5)$$

where A_n is the area of helix blade. The value of N_q determined by Meyerhof (1976) with some reduction can be suitable to involve soil disturbance induced by helical plates. Many references suggest the N_q coefficient of bearing capacity calculated by Eq. (6) (Blessen *et al.* 2017):

$$N_q = 1 + 0.56 (12\phi)^{\phi/54} \quad (6)$$

As seen in Eq. (5), the bearing capacity of helical anchor depends on the friction angle of soil used in the test (N_q), unit weight (γ_i), the embedded depth of helix (H_i), and the area of plates (A_n). Given the use of in the dividual bearing method in design, where the capacity of each plate is assumed, the plate anchor also can be designed by the same method so that the other parameters are not used in designs. In addition, all the soils used in the tests were the same; therefore, the difference in bearing capacity of each anchor depends on the area of the plate and the distance of plate from the wall. In the section of helical and plate anchor properties, the reasons for choosing different types of the anchor and their placing in a group are described in details.

3. LABORATORY EQUIPMENT

In all models, the scale reduction factor of 1/10 was applied. According to the determined scale factor, the whole dimensions were divided by 10 so that a considered retaining wall with 3 × 3 m dimensions was diminished to 30 cm. One of the important member that its stiffness can significantly affect the laboratory results is facing. It is of note that performing no dimensional analysis on the wall facing leads to obtaining incorrect results. In order to construct facing or permanent cover of anchored retaining walls in real condition, the pre-cast concrete sections or integrated concrete casting are adopted. Wood (2014) in his “geotechnical modeling” book after performing the dimensional analysis on four different types of materials aimed at introducing their equivalent thicknesses for using in physical modeling of retaining walls. The real scaled thickness was a 30-cm concrete facing, which has the common thickness in building the real scale retaining walls. Table 1 shows the thickness and modulus of elasticity for four different types of materials introduced by Wood (2014). Considering the performed studies, the facing used in the laboratory, which is similar to 300 mm-thick concrete facing in real condition, was made by 0.9 mm-thick aluminum (Salgado *et al.* 2013). Besides, to prevent any friction and interference among wall facing and lateral

sides of the test box, the width of the facing was considered to be 0.5 mm smaller than 300 mm-width of the box.

To construct a wall with 300 mm length and height, a box was made with length, width, and depth of 100, 30, and 60 cm, respectively. The higher the length and depth of the box were due to prevent the boundary effect on test results and the same width (300 mm) was to ensure having the complete plane strain condition. To observe one side of the prepared retaining walls and take photos during the tests, one side of the box was made of transparent Plexiglass with a thickness of 50 mm. This was because of ensuring its non-deformation and slugging during the loading. The box had calibration points to convert the pixel unit to millimeters and remove the convex of image corners. The schematic of the test box, real condition, and calibration points are illustrated in Fig. 4.

Table 1 The equivalent material of 300 mm-thick concrete facing in the laboratory (Wood 2014)

Facing material	E_m (GPa)	t_m (mm)
Steel	210	0.64
Aluminum	70	0.9
Microconcrete	10	1.75
Polypropylene	0.9	3.9

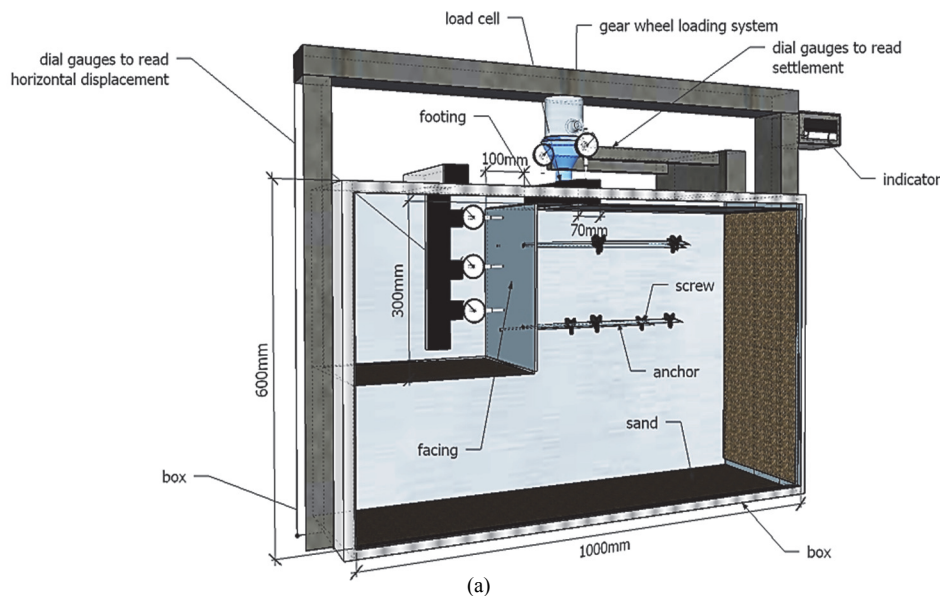


Fig. 4 Test box: (a) schematic image; (b) laboratory environment

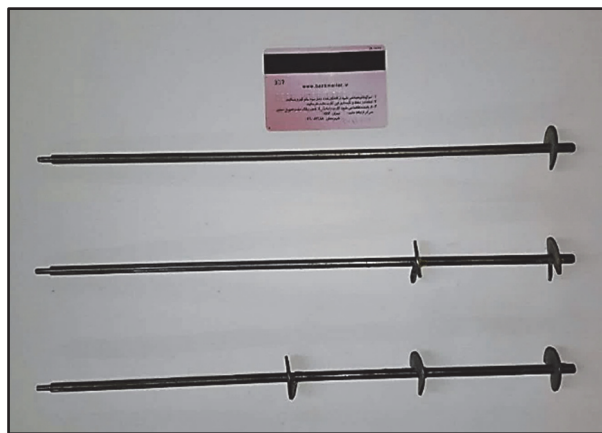
The soil used in this research was the dry sand of Soufian region in East Azerbaijan province of Iran. The soil is classified as SP according to USCS classification. The specifications of this soil are listed in Table 2.

Table 2 Soil properties

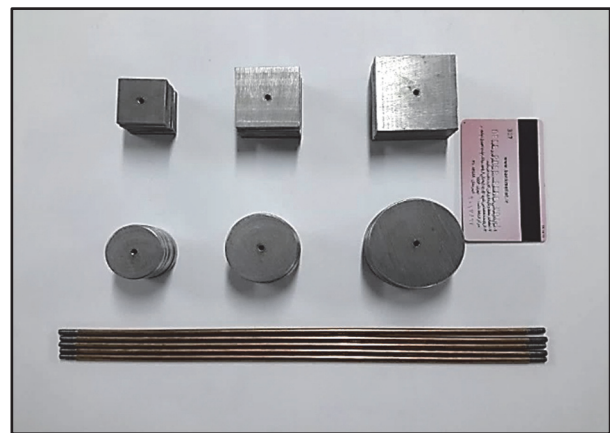
Description	Value
Maximum dry unit weight, $\gamma_{d \max} \left(\frac{kN}{m^3} \right)$	16.76
Minimum dry unit weight, $\gamma_{d \min} \left(\frac{kN}{m^3} \right)$	14.20
Specific gravity, G_s	2.638
Friction angle ϕ (°)	28
Effective grain size, D_{10} (mm)	0.22
Medium grain size, D_{50} (mm)	0.28
Coefficient of uniformity, C_u	1.36
Coefficient of curvature, C_c	0.87
Maximum void ratio, e_{\max}	0.82
Minimum void ratio, e_{\min}	0.54

The helical anchors were fabricated by welding the screws to a metal shaft, while the plate anchors were fabricated through screwing plates to the end of the shafts. The end part of the shafts is threaded to fasten a bolt to them (Fig. 5). The diameter, length, and distance of helices together with shaft diameter and other properties of reinforcements are presented in Table 3. The length of the anchor rod in the plate and helical anchors are 300 and 375 mm, respectively. The closest distance between the helix and failure wedge (critical slip surface) must be three-fold to the helix diameter. Therefore, the minimum length of the helical anchors was selected to be 375 mm with respect to the internal friction angle (ϕ) of the soils, which is the scaled-down of 3.75 m anchor rod (Young 2012). Considering the value of the influence parameter in bearing capacity of anchors, which was obtained by summing area of plates multiplied their distance, the anchors were divided into three groups and compared:

- One-pitch helical anchors, small square, and circular plate anchors
- Double-pitch helical anchors, medium square, and circular plate anchors
- Three-pitch helical anchors, large square, and circular plate anchors



(a)



(b)

Fig. 5 Mechanical ground anchors: (a) three types of fabricated helical anchors; (b) six fabricated plate anchors

Table 3 Specifications of the anchors

Symbol	Type of anchor	Diameter/width of the plate (mm)	The area of plates (mm ²)	The length of anchor rod (mm)	The effective length of bearing capacity (mm)	Influence parameter in bearing capacity (mm ³)	Rod diameter (mm)	The distance of helices (mm)	Group
1H	One-pitch helical anchor	30	706.5	375	375	265,000	4	90	1
2H	Double-pitch helical anchor	30	706.5	375	285-375	466,000	4	90	2
3H	Three-pitch helical anchor	30	706.5	375	195-285-375	604,000	4	90	3
Ss	Small square plate anchor	30	900	300	300	270,000	4	–	1
Sm	Medium square plate anchor	40	1600	300	300	480,000	4	–	2
Sb	Big square plate anchor	50	2500	300	300	750,000	4	–	3
Cs	Small circular plate anchor	33.8	900	300	300	270,000	4	–	1
Cm	Medium circular plate anchor	45	1600	300	300	480,000	4	–	2
Cb	Big circular plate anchor	56.4	2500	300	300	750,000	4	–	3

To have a better understanding, an example of calculating the influence parameter in bearing capacity using Eq. (5) was presented for group 2. The results of other calculations are summarized in Table 3.

$$2H : A_1H_1 + A_2H_2 = 706.5 \times 375 + 706.5 \times 285 = 466,000 \text{ mm}^3$$

$$S_m : A_1H_1 = 1600 \times 300 = 480,000 \text{ mm}^3$$

$$C_m : A_1H_1 = 1600 \times 300 = 480,000 \text{ mm}^3$$

Typically, in most of the projects of constructing permanent retaining walls, the horizontal and vertical distances of reinforcements vary from 1 to 6 m (minimum to maximum). While in conventional soil nail, they are $S_v \times S_h \leq 4$ (S_h is the horizontal space and S_v is the vertical space) (Lazarte *et al.* 2015; Sabatini *et al.* 1999). In addition, the literature review showed that to evaluate the interaction between helical anchors, the appropriate distance between anchors is $1D$ to $6D$ (Albusoda and Abbase 2017; Dong and Zheng 2014; Elsherbiny and El Naggat 2013; Ghaly and Hanna 1994; Ghosh and Samal 2017; Mittal and Mukherjee 2014, 2015). As a result, the horizontal distance of $5D$, which was common in most of the studies, was selected in this work. The same value was also considered for plate anchors. Finally, the horizontal and vertical distances of 1.5 m were chosen for anchor and then by multiplying scale reduction factor of 1/10, the values of 150 mm were obtained for distances of the center to the center of reinforcements in their configurations ($S_v = S_h = 150 \text{ mm}$). Three different anchors configurations on aluminum plates such as square, diamond, and 5-anchor together with the distance of anchors are presented in Fig. 6.

4. MODELING AND TEST PROCESS

In the present work, 9 anchors with three configurations were tested. Totally, 27 tests were performed using a simple factorial method. Generally, the process of constructing mechanical anchor retaining walls is almost identical in all testes and includes backfilling, installation of facing and reinforcement and connecting them to facing in each level. Accordingly, each layer backfilling was done from the bottom of the box until reaching the deployment level of facing. By installing facing in a determined position, the reinforcements were connected to the facing. Then backfilling was done on reinforcements. The process was duplicated for back wall layers to reach the upper reinforcement layers. Finally, the operations of retaining wall construction were ended by re-backfilling until reaching wall crest. It is of note that, in construction steps of the embankment, to establish constant compaction in each test, the thickness of each layer of the embankment was 5 cm and it was kept constant by tamping.

After constructing the wall, the footing was 10 cm away from the wall. In order to have a complete plane strain condition and to prevent the friction between the footing and the sides of the test chamber, the length of the footing was selected 1-mm smaller than the width of the test chamber. Accordingly, the

dimensions of footing were $299 \text{ mm} \times 70 \text{ mm} \times 30 \text{ mm}$ (length \times width \times thickness, respectively). Moreover, the sides of footing were polished to attain the minimum friction between the surface of footing and soil. The applied load using a set of calibrated load cell and indicator, the settlement of footing by vertical strain gauge installed with an equal distance of 70 mm from its center, and the horizontal movement of the wall through three horizontal strain gauge installed with an equal distance of 100 mm in front of facing were read (Fig. 7). The constant strain loading method was used in all tests to reach the maximum precision under a constant loading rate. Accordingly, a dial gauge was mounted on the movable shaft of the loading system to apply the loading in the form of constant 3 mm strain in each step. All six strain gauges have the least count of 0.01 mm.

As mentioned, the backfill soil used in all tests was dry sand, which is classified as poorly graded sand (SP) in accordance with the Unified Soil Classification System (USCS). The density of the backfill was achieved precisely through compacting a fixed mass of sand into a pre-calculated volume of each lift. The unit weight the backfill defined 16 kN/m^3 , which was the same in all experiments. Each test was carried out in 7 stages. In the first step, no load was applied and the first photo was taken from the non-loading soil surface. Then, by applying load during 3 mm constant displacement of the strip footing, the applied force and horizontal wall displacements were respectively read from the indicator and 3 dial gauges. Afterward, the photo was taken from the soil surface and saved. This process was performed in 7 steps to achieve 18 mm settlement of the strip footing. At the end of each loading stage, the photo was taken.

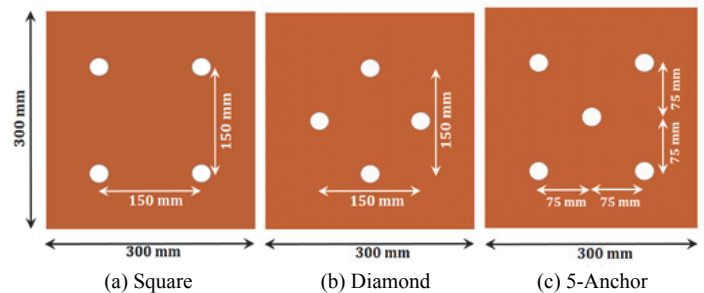


Fig. 6 Anchor configurations

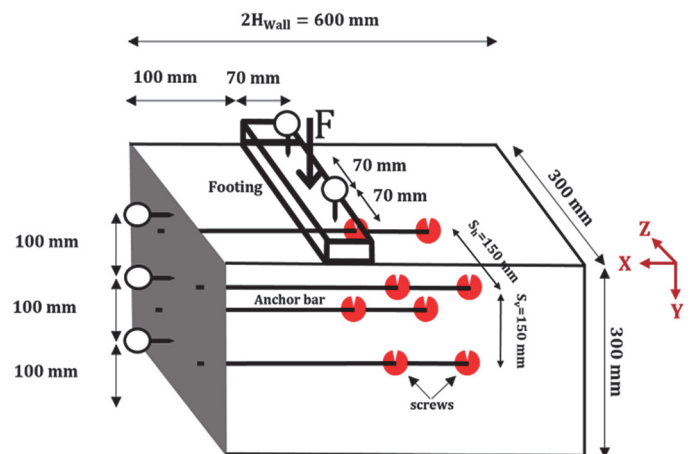


Fig. 7 Schematic diagram of retaining wall

5. DISCUSSION AND EVALUATION

The results of the experiments were presented in three categories including bearing stress of strip footing, the horizontal displacement of the wall, and the shapes of failure wedge. The results were compared and evaluated in terms of changing the type of anchor (helical to the plate), the number of screws in helical anchors, shapes and dimensions of plates in plate anchors, as well as changing the configuration of the reinforcement.

5.1 The Bearing Stress of Footing

The graphs of the absolute settlement of strip footing against bearing stress are shown in Fig. 8 for all tests. Three anchors of group 1 have almost an equal bearing capacity (Figs. 8(a) to 8(c)). However, in all configurations, the circular plate anchor had the maximum bearing stress of the footing. In square configuration and for all anchors, the bearing stress of the footing was almost equal. In this mode, the difference between results is lower than 3% and the best performance belongs to helical anchors. In the diamond configuration, the best performance is related to the circular plate

anchor. In this mode, the difference between the results of helical anchor and circular plate anchor is about 18%. In 5-anchor configuration, the best performance is for circular plate anchor. However, the difference between the results of footing bearing stress of circular plate anchor and the helical anchor is about 12%. The comparison of the first 6 mm loading in graphs showed a better performance of helical anchors, which shows the better locking of these anchors immediately after installing on the wall.

In three anchors of group 2 (Figs. 8(d), 8(e), and 8(f)), the capacity of anchors is almost equal. In square and 5-anchor configurations, the best performance of footing bearing stress in final displacement is for circular plate anchor. The difference between the results of circular plate anchor and helical anchor with the worst performance in square and 5-anchor configuration was 33% and 8%, respectively. In the diamond configuration, the best performance is for the square plate anchor. In this mode, changing the type of reinforcement from helical with the worst performance to square plate anchor led to a 13% increase in footing bearing stress. In this group, in the initial displacements of footing, helical anchors showed better performance compared to plate anchors.

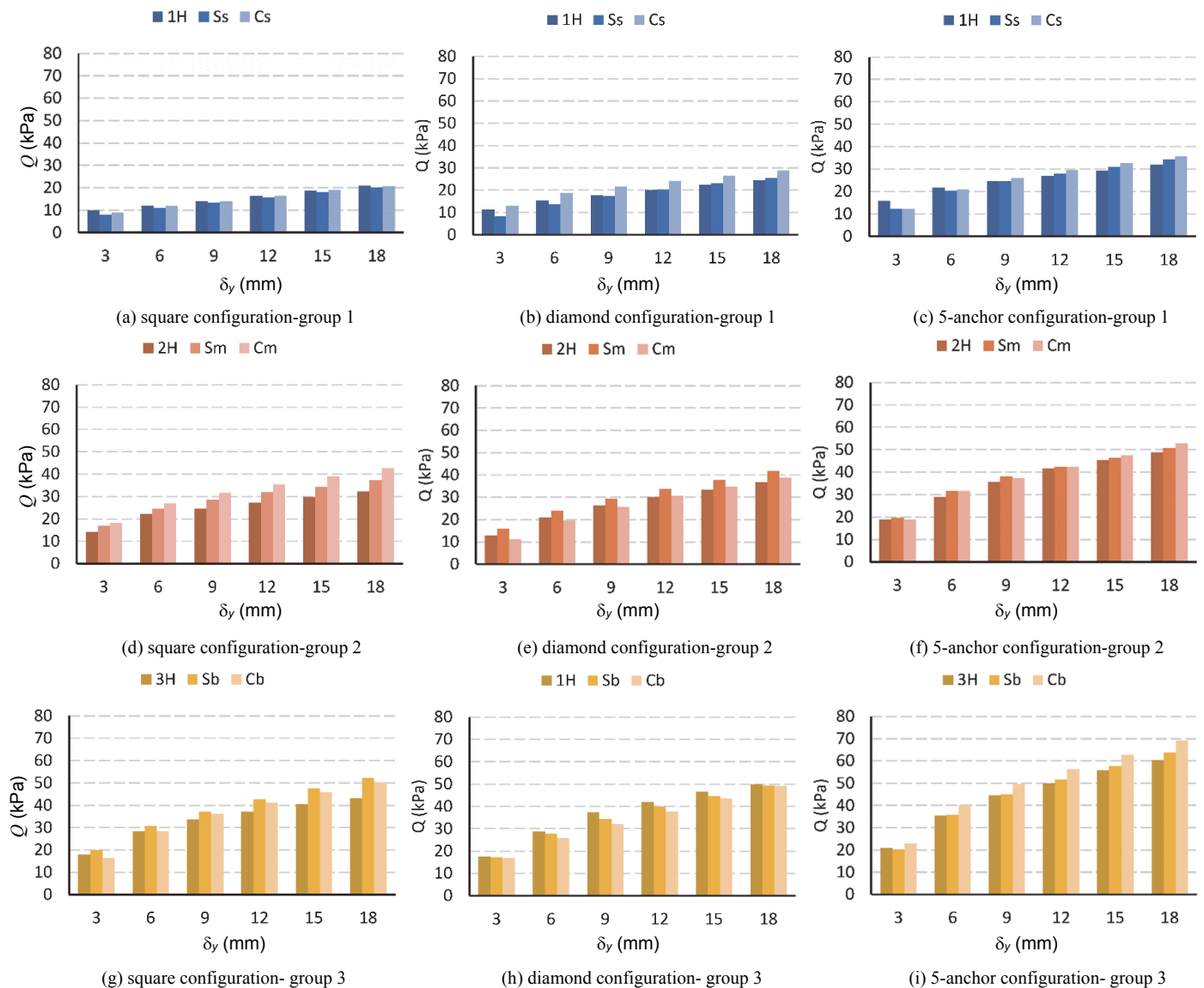


Fig. 8 The settlement of footing against bearing stress for square, diamond, and 5-anchor configurations

As seen in Table 3, the effective parameter in bearing capacity of helical anchors of group 3 is 604,000 mm³, while in plate anchors of group 3, the parameter equals to 750,000 mm³. Therefore, the bearing capacity of helical anchors of group 3 was 4/5 of plate anchors (Figs. 8g, 8h, and 8i). However, no significant difference was observed in the footing bearing of 3-pitch helical anchors and plate anchors. Especially, in a diamond configuration, the helical anchors had almost the same condition with plate anchors. To have a better evaluation in anchors of group 3, a comparison was made between the bearing stress of the footing in two configurations of 5-helical anchors and 4-plate anchors.

In this mode, the change of footing bearing stress was about 1% and the best performance was for helical anchors. In the square configuration, the best performance was observed in square plate anchor and the difference between its result and that of the helical anchor with the worst performance was about 20%. In 5-anchor configuration, the best performance was for circular plate anchor and the difference between its results and that of the helical anchor with the worst performance was about 14%. Generally, it should be noted that the maximum effect of changing anchor on footing bearing stress was observed in a square configuration and group 2, where changing the helical anchor to circular plate one led to a 33% increase in bearing stress.

In anchors of group 1, which had the minimum bearing capacity, in all configurations, 33% to 50% of total bearing stress of footing occurred in the first step of settlement. In the anchors of group 2, by increasing the bearing capacity, in all configurations, almost 29% to 46% of total bearing stress of footing occurred in the first step of settlement. Finally, in the anchors of group 3, which had the maximum bearing capacity, in all configuration, almost 32% to 41% of total bearing stress of footing occurred in the first step of settlement. It was indicated that an increase in bearing capacity of anchors, the applied bearing stress on the footing are dispersed in different steps. Moreover, in all anchors and configurations, by increasing the bearing capacity, the effect of footing bearing stress is reduced in the first step. Besides, in all configurations and anchors, the maximum footing bearing stress occurs in the first step of settlement. In addition, by increasing the settlement steps, the increase in footing bearing stress had a descending trend.

In Fig. 9, a comparison is made between the diagrams of changing anchor configuration and footing bearing stress. As seen, in these three configurations, the effect of changing the number of screw and plate dimensions on bearing stress is higher than changing the configuration. However, despite having the same number of the anchor, the diamond configuration showed better performance compared to square one and almost in all cases, this configuration had higher bearing stress than the square one. The results of this mode are in agreement with the checked configuration in the regulation of common nails (Lazarte *et al.* 2015).

As presented in Fig. 9, changing the number of helices and plate dimensions significantly affects the bearing stress. Hence, an increase in the number of helices from single to double in the square, diamond, and 5-anchor configurations respectively leads to 55%, 50%, and 53% increase in bearing stress. Also, increasing the number of helices from 2 to 3 in the square, diamond, and 5-anchor configurations respectively results in 34%, 36%, and 24% increase in bearing stress. Generally, although increasing the number of helices from 1 to 2 leads to a 53% increase in bearing stress, increasing from 2 to 3 only results in a 31% increase in bearing stress. It is predicted that the increasing rate of bearing capacity of reinforcements is significantly decreased by increasing the number of helices and lose its

positive effect. Hence, in the cases where there is a need for numerous bearing capacity of the helical anchor, another method should be employed, instead of increasing unrestricted helices.

In circular plate anchors with square, diamond, and 5-anchor configurations, also an increase in plate diameter from small to medium lead to 106%, 34%, and 48% increase in footing bearing stress, respectively. By changing the plate dimensions of the circular plates with square, diamond, and 5-anchor configurations, from medium to large, respectively, 18%, 27%, and 31% increase in bearing stress occurs. In square plate anchor, an increase in plate width and change of anchor type from small to medium result in 84%, 64%, and 48% increase in bearing stress in the square, diamond, and 5-anchor configurations, respectively. Changing the type of square plate anchor with square, diamond, and 5-anchor configurations from medium to large lead to 41%, 18%, and 26% increase in footing bearing stress. On the other hand, in plate anchors, by increasing the dimensions of the plates, the increasing rate of bearing stress is decreased. This is while the increasing rate of plate dimensions from medium to large was more than that from small to medium.

Generally, in all anchors, increasing the dimensions or the number of helices in square and diamond configuration had a higher effect on increasing the bearing stress compared to 5-anchor configuration. In addition, the results indicated that in 5-anchor configuration, the anchors of each group showed almost the same results and the difference between the results of this configuration with others was more limited.

Adding an anchor to the diamond configuration and converting it to 5-anchor configuration led to an increase in footing bearing stress. In terms of the footing bearing stress, the comparison was made between 5-anchor configuration with three-pitch helical anchor and 4-anchor configuration with large plate anchor. The dimensions of helical and plate anchors were selected by considering obtaining the equivalent bearing capacity for 5 three-pitch helical anchors and 4 plate anchors with large size. In the case of large plate anchors with square and diamond configurations of the reinforcements, the bearing stress of footing varies from 49.2 to 52.3 kPa, while it is 60.4 kPa in 5 three-pitch helical anchors.

As a general result, in all configurations and using anchors with identical bearing capacity, the best performance in footing bearing was observed in plate anchors with low and medium bearing capacity, while the best performance in footing bearing under the use of anchors with high bearing capacity was for helical anchors.

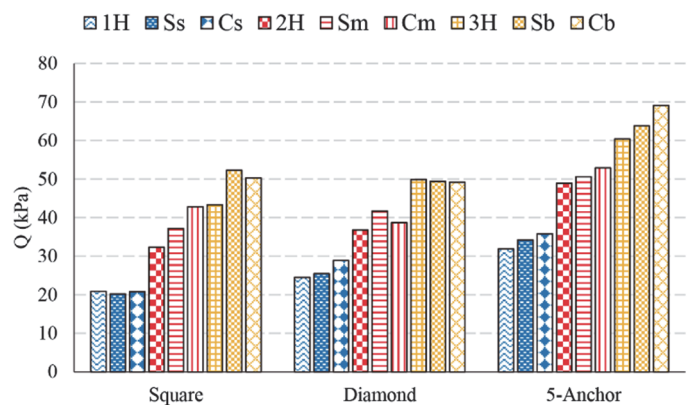


Fig. 9 The curves of configurations against bearing stress of footing

5.2 Wall Displacement

The graphs of strip footing absolute settlement against the horizontal displacement of the wall are illustrated in Fig. 10. In anchors of group 1 (Figs. 10(a), 10(b), and 10(c)) with the same bearing capacity, changing the type of anchors from helical to plate anchor lead to decreasing the horizontal displacement of wall. The reduction was in the ranges of 13% to 27% for changing configuration and anchor type. In all stages of footing displacement, the performance of plate anchors in controlling the wall crest displacement was better than helical anchors. The wall crest displacement rates in two circular and square plate anchors of group 1 were almost equal and changing the type of plate anchor had no significant effect on displacement. The change of wall displacement by changing the plate from circular to the square was in the range of 1% to 10%.

In the anchors of group 2 (Figs. 10(d) to 10(f)), which had the almost identical bearing capacity, the plate anchors showed better

performance in almost all configurations. In this case, the difference in results was lower than that of group 1 and the change in the type of anchor from helical to the plate had less effect on displacements control. In the diamond configuration, the performance of two-pitch helical anchor was better than circular plate anchor and it led to less displacement.

In group 3 (Figs. 10(g) to 10(i)), changing the type of anchor from helical to plate anchor significantly affect the displacements control. All configuration of plate anchors showed better performance compared to helical anchors in term of wall displacement control because of lower bearing capacity of helical anchors of group 3 than plate anchors. To have a better evaluation in anchors of group 3, a comparison was made between the horizontal displacement of the wall in two configurations of 5-helical anchors and 4-plate anchors. It is of note that, changing the type of anchor in group 3 had the maximum effect on wall displacement and had less impact on bearing stress of footing.

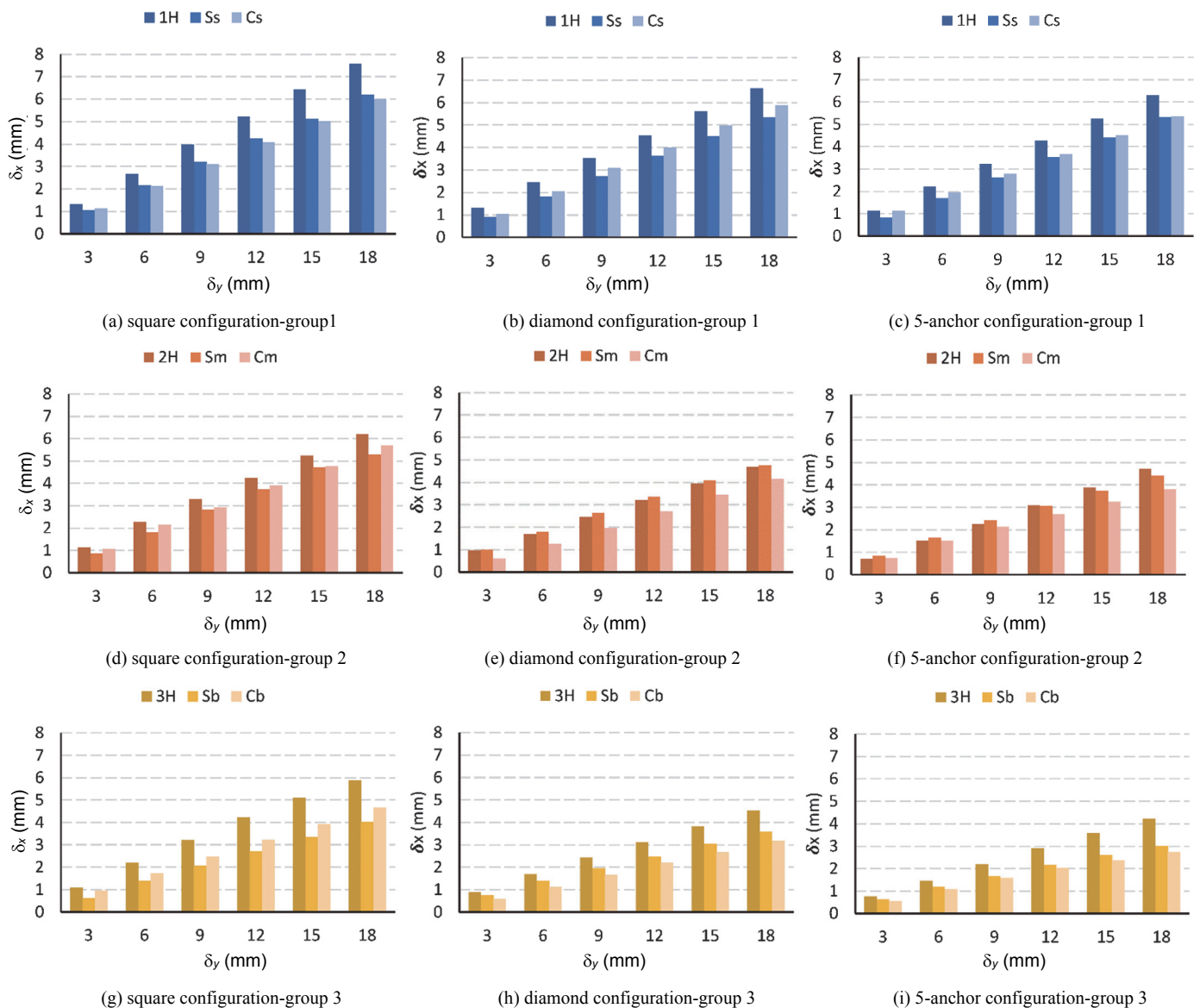


Fig. 10 The graphs of configuration against wall displacement (the horizontal displacement of the crest δ_x against the settlement of footing δ_y)

In Fig. 11, the horizontal wall crest displacements of different configurations are presented. As seen, changing the number of helices and dimensions of plate anchors significantly affects the horizontal displacement of the wall and it is more obvious in diamond configuration compared to square one. In the square, diamond, and 5-anchor configuration, by changing the number of the helices from 1 to 2, the wall crest displacement respectively was reduced by 18%, 29%, and 25%. In the square, diamond, and 5-anchor, changing the number of helices from 2 to 3 leads to 5%, 4%, and 11% reduction in wall crest displacement. Therefore, an increase in the number of pitches results in a decrease in the reduction rate of displacement. It can be concluded that the more increase in the number of helices (more than 3) has no significant effect on increasing the reinforcement fixing and wall stability.

In square plate anchors with square, diamond, and 5-anchor configurations, 15%, 11%, and 17% decrease in wall displacement respectively occurred by changing plate size from small to medium, while by changing plate size from medium to big, 23%, 25%, and 32% decrease in wall displacement respectively were observed. In circular plate anchors with square, diamond, and 5-anchor configurations, 5%, 29%, and 29% reductions in wall displacement respectively occurred by changing plate size from small to medium, while by changing plate size from medium to big, 18%, 23%, and 28% reductions in wall displacement respectively were observed. Almost size changing from small to medium and medium to large in plate anchors were the same. However, in most of the plate anchors and configurations, the reduction rate of wall displacement showed a growing trend by increasing the plate size of plate anchor.

In single, double, and three-pitch anchors, changing the square configuration to diamond led to 13%, 24%, and 23% reductions in wall crest displacement, respectively. While, in single, double, and three-pitch anchor, adding an anchor to the diamond configuration (5-anchor) resulted in 5%, 0%, and 7% reductions in displacement, respectively. In square plate anchors, changing the square to the diamond configuration for small, medium, and large plates led to 14%, 10%, and 11% reduction in wall displacement, while changing the diamond configuration to 5-anchor caused 1%, 7%, and 16% reduction, respectively. In circular plate anchors, changing the square to the diamond configuration for small, medium, and large plates resulted in 2%, 27%, and 32% reduction in wall displacement. However, in the same anchors, changing the diamond configuration to 5-anchor resulted in 9%, 9%, and 14% reductions in wall displacement for small, medium, and large plates, respectively.

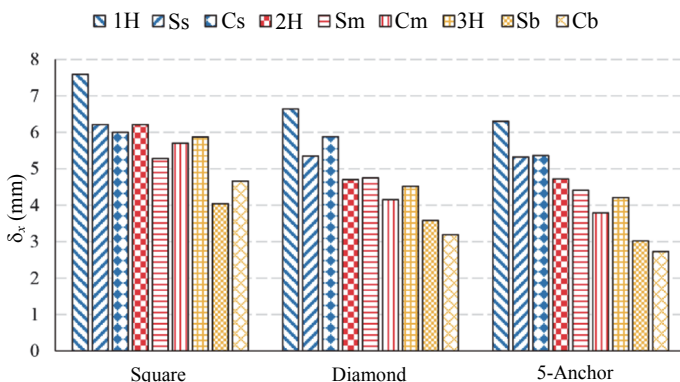


Fig. 11 The graphs of configurations against the horizontal displacement of the wall (δ_x)

Generally, changing the configuration of anchors had a significant effect on wall displacement, even higher than increasing the number of anchors. According to the results, the diamond configuration in all types of anchor showed better performance in controlling wall displacement compared to the square configuration. Besides, increasing the number of the pitch in helical anchors and the dimensions of the plate in plate anchors affected the bearing stress of footing more than wall displacements control. In the case that displacements control is necessary, post-tensioning the anchors can be a proper approach.

In terms of the wall displacement, the comparison was made between 5-anchor configuration with three-pitch helical anchor and 4-anchor configuration with large plate anchor. The dimensions of helical and plate anchors were selected by considering obtaining the equivalent bearing capacity for 5 three-pitch helical anchor and 4 plate anchors with large size. In the case of large plate anchors with square and diamond configurations, the wall crest displacement varies from 3.19 to 4.04 mm, while it is 4.21 mm in the 5 three-pitch helical anchors. It can be concluded that the direct-embedded plate anchors have a better performance in controlling the wall crest displacement compared to helical anchors under the same bearing capacity condition.

As a result, it can be stated that in all groups of anchors and configurations, the plate anchors showed a better performance in controlling the horizontal wall crest displacements compared to helical anchors. The results of the displacement of wall crest and footing bearing stress conducted on 27 tests are presented in Table 4.

5.3 Failure Wedge

To determine the failure wedge formation, photogrammetry and particle image velocimetry (PIV) methods were used. Continuous photos are taken from soil surface during deformation by a digital camera and then soil deformation is evaluated between each pair of photos through the PIV analysis. The images were taken using the Canon PowerShot G10 equipped with a CCD sensor. To prevent camera displacement, all photos were provided by remote capture and pc software. Then the images were analyzed through PIV method using GeoPIV module. The output of this code is a two-dimensional matrix with u and v components, which represent horizontal and vertical components of the displacement vector in each point, respectively. This code was written by White *et al.* (2003) as an M-file in MATLAB software. Figs. 12, 13, and 14 show the images for the shear strain of particles in the critical sliding surface for group 1 to 3 anchors. The first right column represents the range of strains in soil particles.

As seen in Figs. 12 and 13, in all anchors of group 1 and 2, failure wedges were completely formed. However, in group 3, due to an increase in bearing capacity of anchors (Fig. 14), a very limited failure wedge was formed in walls of this group. In all groups, the expansion of slip surface formed in helical anchors was more than plate anchors. Since the circular plate anchors have lower shear strains and expansion compared to square plate anchors, the failure wedge is formed more limited and imperfect. It shows the performance of circular plate anchors is better than square plate anchors.

As seen in Figs. 12, 13, and 14, in helical anchors, the failure wedge is passed the wall heel, while in plate anchor it is passed upper the wall heel. Almost in all anchors, changing square to diamond and diamond to 5-anchor configuration leads to a reduction in shear strain and failure wedge expansion. It can be concluded that diamond configuration has better performance compared to the square configuration.

Table 4 The displacement of wall crest and footing bearing stress in performed tests

Group	Type of anchor	Configuration	The horizontal displacement of the wall (mm)	Bearing stress of footing (kPa)
1	One-pitch helical anchor	Square	7.6	20.9
	Small square plate anchor	Square	6.2	20.2
	Small circular plate anchor	Square	6.0	20.8
1	One-pitch helical anchor	Diamond	6.6	24.5
	Small square plate anchor	Diamond	5.4	25.5
	Small circular plate anchor	Diamond	5.9	28.9
1	One-pitch helical anchor	5-Anchor	6.3	31.9
	Small square plate anchor	5-Anchor	5.3	34.2
	Small circular plate anchor	5-Anchor	5.4	35.8
2	Double-pitch helical anchor	Square	6.2	32.3
	Medium square plate anchor	Square	5.3	37.2
	Medium circular plate anchor	Square	5.7	42.8
2	Double-pitch helical anchor	Diamond	4.7	36.8
	Medium square plate anchor	Diamond	4.8	41.7
	Medium circular plate anchor	Diamond	4.2	38.7
2	Double-pitch helical anchor	5-Anchor	4.7	48.9
	Medium square plate anchor	5-Anchor	4.4	50.6
	Medium circular plate anchor	5-Anchor	3.8	52.9
3	Three-pitch helical anchor	Square	5.9	43.3
	Big square plate anchor	Square	4.0	52.3
	Big circular plate anchor	Square	4.7	50.3
3	Three-pitch helical anchor	Diamond	4.5	49.9
	Big square plate anchor	Diamond	3.6	49.4
	Big circular plate anchor	Diamond	3.2	49.2
3	Three-pitch helical anchor	5-Anchor	4.2	60.4
	Big square plate anchor	5-Anchor	3.0	63.8
	Big circular plate anchor	5-Anchor	2.7	69.1

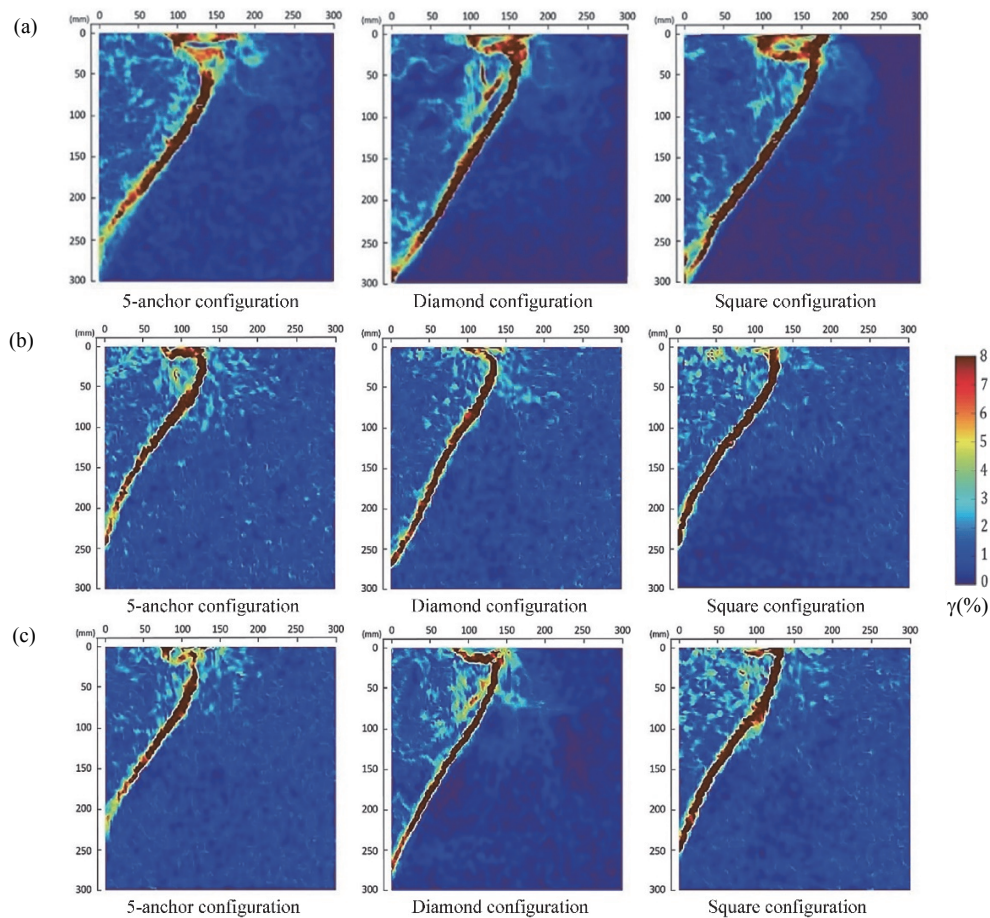


Fig. 12 The output of PIV: (a) single-pitch helical anchor; (b) small square plate anchor; (c) small circular plate anchor

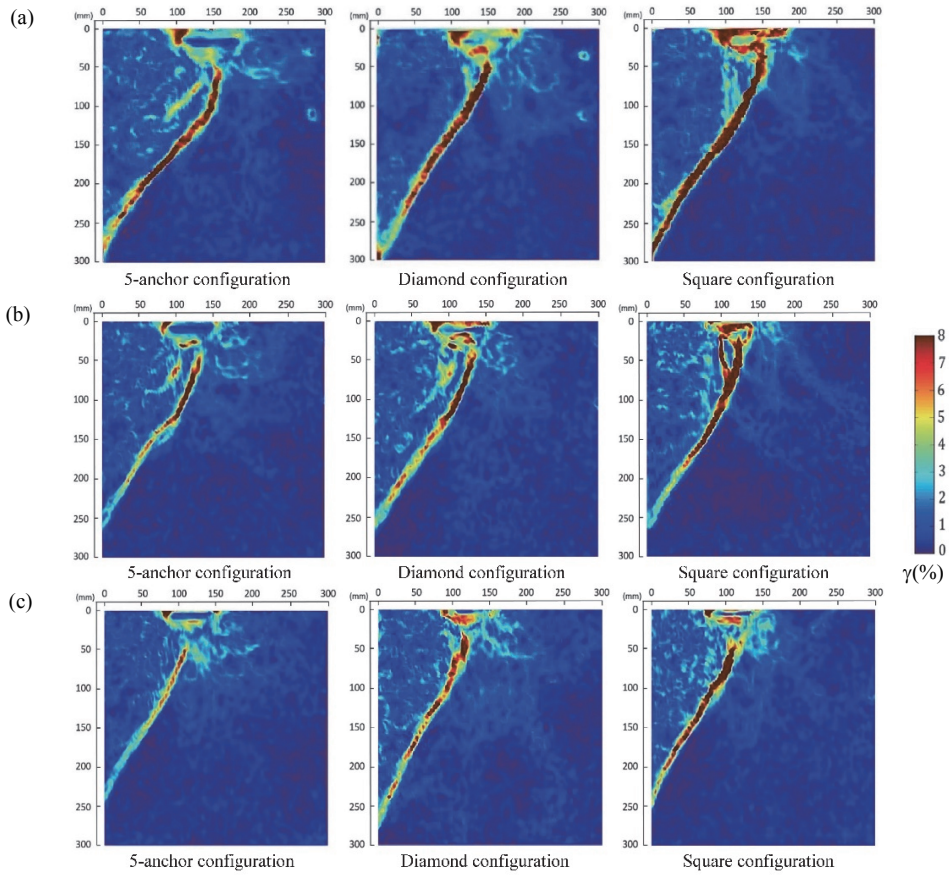


Fig. 13 The output of PIV: (a) double-pitch helical anchor; (b) medium square plate anchor; (c) medium circular plate anchor

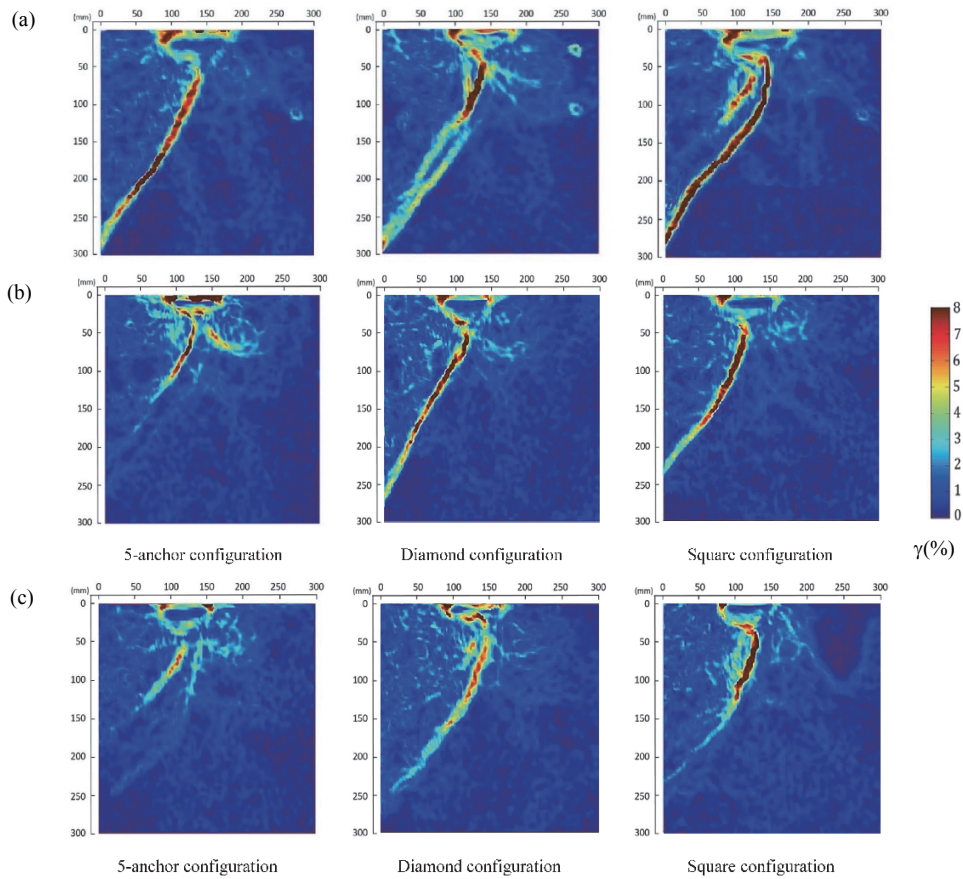


Fig. 14 The output of PIV: (a) three-pitch helical anchor; (b) large square plate anchor; (c) large circular plate anchor

The evaluation of failure wedge revealed that the distance of sliding surface from wall crest was the same in all tests and it was started from the outer edge of footing (the edge far from facing). In the diamond configuration, almost a linear wedge was formed in all anchors. In the square and 5-anchor configurations, the failure wedge is an almost logarithmic spiral. Finally, as obvious in Figs. 12, 13, and 14, an increase in the number of helices and dimensions of the plate in anchors result in a decrease in shear strains.

5.4 Mechanism of Wall Deformation

The schematic of wall deformation resulting from the separate sum of three extensometers available on the height of the wall for anchors of group 1 is shown in Fig. 15. In 5-anchor and diamond configurations, the maximum displacements were observed on the crest of the wall and toward downside of the wall, the displacement was reduced. In these configurations, the wall deformation mechanism was almost linear. The diamond configuration with one reinforcement less showed less difference in displacements with 5-anchor configuration. In the square configuration, a sagging was observed in the middle of the wall due to the large non-reinforced opening. Therefore, the maximum displacement occurs in the middle of the wall, which shows the inappropriate configuration and distribution of reinforcements on the wall. In all configurations, wall footing showed some displacement. In order to prevent displacement, the wall can be implemented as rooted.

6. CONCLUSIONS

In the present study, a set of experiments were conducted to evaluate the effect of changing the dimensions and shape of the plate anchors, the number of pitches of helical anchors, and reinforcement's configuration on wall displacement, footing bearing stress, and shapes of failure wedge. The results are as follows:

1. Increasing the number of pitches from single to double and changing the size of circular and square plate anchors from small to medium led to a 60% increase in footing bearing stress. In comparison, increasing the number of pitches from double to three and changing the size of circular and square plate anchors from medium to large resulted in a 29%

increase in footing bearing stress. It is predicted that this ascending trend in the bearing stress of the footing is continued by increasing the number of helices and the size of plates and more increase results in losing its positive effect. Therefore, to increase the bearing capacity of footing, other parameters such as the length of the anchor or its number should be adjusted.

2. In most of the anchors, in square and diamond configurations, increasing the dimensions or the number of helices had a higher effect on increasing footing bearing stress compared to 5-anchor configuration. In addition, the results showed that in 5-anchor configuration, the anchors of all groups showed the same results and the difference between the results was lower than other configurations.
3. In large plate anchors with square and diamond configuration, the footing bearing stress and wall crest displacement are 49.2 ~ 52.3 kPa and 3.19 ~ 4.04 mm, respectively. Moreover, in the three-pitch helical anchor with 5-anchor configuration, the bearing stress and wall displacement are respectively 60.4 kPa and 4.21 mm. Therefore, when the anchors have the identical bearing capacity, if the footing bearing is limited in design, we can use helical anchor but if the crest displacement control has more importance, the use of plate anchors are suggested.
4. In different configurations, changing the helical anchors from single to double pitch decrease the wall crest displacement by 24%. However, changing the helical anchors from double-pitch to three-pitch in different configurations leads to a 7% reduction in wall displacement. Therefore, a further increase in the number of pitches in helical anchors results in decreasing the effect of the number of helices on controlling wall crest displacement.
5. In most of the plate anchors and configurations, the reduction rate of wall crest displacement has a growing trend by increasing the area of plate anchor.
6. In helical anchors, increasing the number of pitches and dimensions of the plate in plate anchors affect the bearing stress of footing more than wall displacement control. Where wall displacement control is needed, post-tensioning of anchors can be a good method.

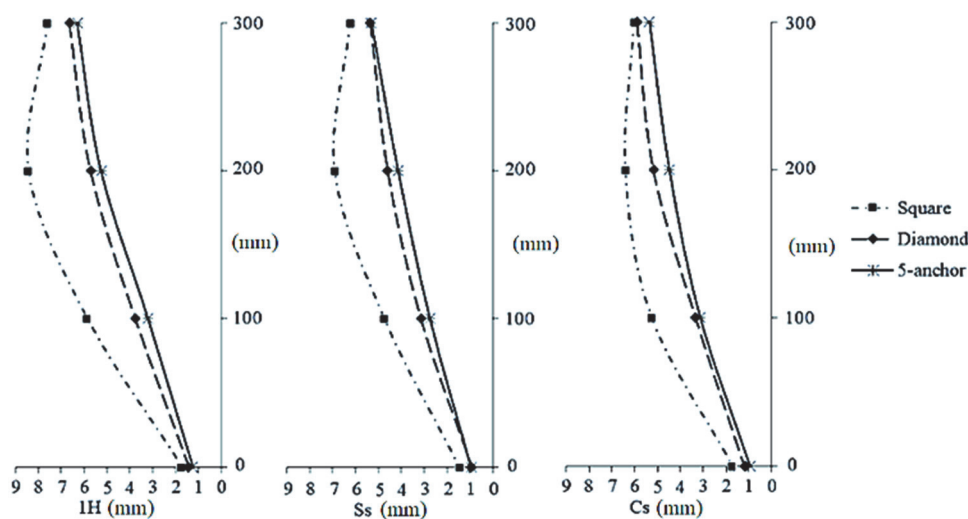


Fig. 15 The schematic of wall deformation

7. In both diamond and square configurations, the number of anchors is the same. However, diamond configuration showed better performance in controlling wall crest displacement compared to the square configuration. This issue affected the reduction of shear strain and its expansion. Moreover, the effect of changing the configuration on controlling the wall crest displacement was higher than that of increasing an anchor.
8. In all anchors, the expansion of failure wedge in helical anchors was more than plate anchors. The performance of circular and square plate anchors in the formation of failure wedge and expansion of slip surface was almost identical. However, the circular plate anchors slightly showed better performance against the formation of failure wedge.

FUNDING

The authors received no funding for this work.

DATA AVAILABILITY

All data and/or computer codes used/generated in this study are included in this paper.

REFERENCES

- Albusoda, B.S. and Abbase, H.O. (2017). "Performance assessment of single and group of helical piles embedded in expansive soil." *International Journal of Geo-Engineering*, **8**(1), 25. <https://doi.org/10.1186/s40703-017-0063-x>
- Blessen, J., Dearthoff, D., Dikeman, R., Kortan, J., Malone, J., Olson, K., and Waltz, N. (2017). "Helical Piles and Anchors-Hydraulically Driven Push Piers — Polyurethane Injection." *Supplemental Support Systems. Supportworks, Ed., Third Ed.*
- Boussinesq, J. (1885). *Application des Potentiels à l'Etude de l'Equilibre et du Mouvement des Solides*. Gauthier-Villars, France.
- Clemence, S. and Lutenegeger, A. (2015). "Industry survey of state of practice for helical piles and tiebacks." *DFI Journal-The Journal of the Deep Foundations Institute*, **9**(1), 21-41. <https://doi.org/10.1179/1937525514Y.0000000007>
- Dearthoff, D., Moeller, M., and Walt, E. (2010). "Results of an instrumented helical soil nail wall." *Proceedings of the Earth Retention Conference*, **3**, 262-269. [https://doi.org/10.1061/41128\(384\)24](https://doi.org/10.1061/41128(384)24)
- Dong, T.W. and Zheng, Y.R. (2014). "Limit analysis of vertical anti-pulling screw pile group under inclined loading on 3D elastic-plastic finite element strength reduction method." *Journal of Central South University*, **21**(3), 1165-1175. <https://doi.org/10.1007/s11771-014-2050-0>
- El Sawwaf, M. and Nazir, A. (2006). "The effect of soil reinforcement on pullout resistance of an existing vertical anchor plate in sand." *Computers and Geotechnics*, **33**(3), 167-176. <https://doi.org/10.1016/j.compgeo.2006.04.001>
- Elsherbiny, Z. and El Naggar, M. (2013). "The performance of helical pile groups under compressive loads: a numerical investigation." *Proceedings of the 18th International Conference on Soil Mechanics and Geotechnical Engineering*, Paris.
- Geddes, J.D. and Murray, E.J. (1996). "Plate anchor groups pulled vertically in sand." *Journal of Geotechnical Engineering*, ASCE, **122**(7), 509-516. [https://doi.org/10.1061/\(ASCE\)0733-9410\(1996\)122:7\(509\)](https://doi.org/10.1061/(ASCE)0733-9410(1996)122:7(509))
- Ghaly, A. and Hanna, A. (1994). "Model investigation of the performance of single anchors and groups of anchors." *Canadian Geotechnical Journal*, **31**(2), 273-284. <https://doi.org/10.1139/94-032>
- Ghosh, P. and Samal, S. (2017). "Interaction effect of group of helical anchors in cohesive soil using finite element analysis." *Geotechnical and Geological Engineering*, **35**(4), 1475-1490. <https://doi.org/10.1007/s10706-017-0188-x>
- Hanna, A., Foriero, A., and Ayadat, T. (2015). "Pullout capacity of inclined shallow single anchor plate in sand." *Indian Geotechnical Journal*, **45**(1), 110-120. <https://doi.org/10.1007/s40098-014-0113-7>
- Hoyt, R. (1989). "Uplift capacity of helical anchors in soil." *Proceedings of 12th International Conference on Soil Mechanics and Foundation Engineering*, 1019-1022.
- Lazarte, C.A., Robinson, H., and Gómez J.E. et al (2015). *Soil Nail Walls Reference Manual*. (No. FHWA-NHI-14-007).
- Lutenegeger, A. (2011). "Behavior of multi-helix screw anchors in sand." *Proceedings of the 14th Pan-American Conference on Soil Mechanics and Geotechnical Engineering*, Toronto, Ont.
- Mittal, S. and Mukherjee, S. (2014). "Vertical pullout capacity of a group of helical screw anchors in sand: An empirical approach." *Indian Geotechnical Journal*, **44**(4), 480-488. <https://doi.org/10.1007/s40098-014-0099-1>
- Mittal, S. and Mukherjee, S. (2015). "Behaviour of group of helical screw anchors under compressive loads." *Geotechnical and Geological Engineering*, **33**(3), 575-592. <https://doi.org/10.1007/s10706-015-9841-4>
- Moghadam, M.J., Zad, A., Mehrannia, N., and Dastaran, N. (2018a). "Experimental evaluation of mechanically stabilized earth walls with recycled crumb rubbers." *Journal of Rock Mechanics and Geotechnical Engineering*, **10**(5), 947-957. <https://doi.org/10.1016/j.jrmge.2018.04.012>
- Moghadam, M.J., Zad, A., Mehrannia, N., and Dastaran, N. (2018b). "Experimental study on the performance of plate anchor retaining walls." *International Journal of Physical Modelling in Geotechnics*, **19**(3), 128-140. <https://doi.org/10.1680/jphmg.17.00040>
- Perko, H.A. (1999). "Summary of earth retaining methods utilizing helical anchors." *Magnum Piering Technical Reference Guide, Engineering Analysis*, Section 3. Cincinnati, OH: Magnum Piering, Inc.
- Perko, H.A. (2009). *Helical Piles: A Practical Guide to Design and Installation*. John Wiley & Sons.
- Sabatini, P., Pass, D., and Bachus, R.C. (1999). *Ground Anchors and Anchored Systems*. No. FHWA/IF-99-015. United States. Federal Highway Administration. Office of Bridge Technology.
- Salgado, R., Yoon, S., and Zia, S.N. (2013). *Construction of Tire Shreds Test Embankment*. Joint Transportation Research Program, Technical Report N: FHWA/IN/JTRP-2002/35. Available at: <http://docs.lib.purdue.edu/jtrp/42/>. Accessed 11Feb
- Sharma, M., Samanta, M., and Sarkar, S. (2017). "Laboratory study on pullout capacity of helical soil nail in cohesionless soil." *Canadian Geotechnical Journal*, **54**(10), 1482-1495. <https://doi.org/10.1139/cgj-2016-0243>
- Stephenson, R.W. (2003). *Design and Installation of Torque Anchors for Tiebacks and Foundations*. Missouri University of Science and Technology, Rolla, 45p.
- Tokhi, H., Ren, G., and Li, J. (2016). "Laboratory study of a new screw nail and its interaction in sand." *Computers and Geotechnics*, **78**, 144-154.

- <https://doi.org/10.1016/j.compgeo.2016.05.009>
Tokhi, H., Ren, G., and Li, J. (2017). "Laboratory pullout resistance of a new screw soil nail in residual soil." *Canadian Geotechnical Journal*, **55**(5), 609-619.
<https://doi.org/10.1139/cgj-2017-0048>
- White, D., Take, W., and Bolton, M. (2003). "Soil deformation measurement using particle image velocimetry (PIV) and photogrammetry." *Geotechnique*, **53**(7), 619-631.
- <https://doi.org/10.1680/geot.2003.53.7.619>
Wood, D.M. (2014). *Geotechnical Modelling*. CRC Press.
- Young, J.J.M. (2012). *Uplift Capacity and Displacement of Helical Anchors in Cohesive Soil*. Master Thesis, School of Civil and Construction Engineering, Oregon State University, Corvallis, OR. 177 pp. Available at: <http://hdl.handle.net/1957/29487>. Date of access: 25.06.2014